EXHIBIT B

A Comprehensive Guide for the Accurate Classification of Murine Hair Follicles in Distinct Hair Cycle Stages

Sven Müller-Röver, Bori Handjiski,* Carina van der Veen,* Stefan Eichmüller,† Kerstin Foitzik, Ian A. McKay,‡ Kurt S. Stenn,§ and Ralf Paus

Department of Dermatology, University Hospital Eppendorf, University of Hamburg, Hamburg, Germany; *Department of Dermatology, Charité, Humboldt University, Berlin, Germany; †Department of Dermatology, Klinikum Mannheim, University of Heidelberg, Mannheim, Germany; ‡Center for Cutaneous Research, Queen Mary and Westfield College, University of London, U.K.; §Johnson and Johnson Skin Biology TRC, Skillman, New Jersey, U.S.A.

Numerous strains of mice with defined mutations display pronounced abnormalities of hair follicle cycling, even in the absence of overt alterations of the skin and hair phenotype; however, in order to recognize even subtle, hair cycle-related abnormalities, it is critically important to be able to determine accurately and classify the major stages of the normal murine hair cycle. In this comprehensive guide, we present pragmatic basic and auxiliary criteria for recognizing key stages of hair follicle growth (anagen), regression (catagen) and quiescence (telogen) in C57BL/6NCrlBR mice, which are largely based on previous work from other authors. For each stage, a schematic drawing and representative micrographs are provided in order to illustrate these criteria. The basic criteria can be employed for all mouse strains and require only routine histochemical techniques. The auxiliary criteria depend on the immunohistochemical analysis of three markers (interleukin-1 receptor type I, transforming growth factor-β receptor type II, and neural cell-adhesion molecule), which allow a refined analysis of anatomical hair follicle compartments during all hair cycle stages. In contrast to prior staging systems, we suggest dividing anagen III into three distinct substages, based on morphologic differences, onset and progression of melanogenesis, and the position of the dermal papilla in the subcutis. The computer-generated schematic representations of each stage are presented with the aim of standardizing reports on follicular gene and protein expression patterns. This guide should become a useful tool when screening new mouse mutants or mice treated with pharmaceuticals for discrete morphologic abnormalities of hair follicle cycling in a highly reproducible, easily applicable, and quantifiable manner. ***Key words: alkaline phosphatase/anagen/catagen/dermal papilla/telogen.*** ***J Invest Dermatol 117:3–15, 2001***

The hair follicle (HF) is a highly sensitive mini-organ whose cyclic transformations from phases of rapid growth (anagen), via apoptosis-driven regression (catagen) to relative quiescence (telogen) (Dry, 1926) are profoundly influenced by numerous growth factors, cytokines, hormones, neuropeptides, and pharmaceutical products (for review see Paus, 1996, 1998; Stenn *et al*, 1996, 1998; Paus and Cotsarelis, 1999). These manipulations of HF cycling are of substantial interest to an ever-growing community of life scientists and physicians. Yet, it is far from trivial to assess accurately and quantify alterations in HF cycling.

In addition to the human hair cycle (Kligman, 1959), the main three phases of the HF cycle have been described and investigated in most pigmented mouse strains, albino mice, and in some mouse mutants (Dry, 1926; Chase *et al*, 1951; Chase, 1954; Orwin *et al*, 1967; Sundberg, 1994; Panteleyev *et al*, 1998, 1999). Decades ago, landmark publications by Chase *et al* (1951), Chase (1954), and Straile *et al* (1961) defined key parameters for the recognition of distinct stages of the murine hair cycle. For nearly 50 y, these publications have been used as key references for HF classification, although none of them offers a comprehensive, unified classification scheme for the complete hair cycle; however, describing even subtle hair cycle changes has become of paramount importance to the analysis of mouse mutants, transgenic and knockout mice, and to the analysis of experimental drug effects in mice. The present guide aims to offer scientists with an interest in hair research an updated and pragmatic approach to rapid, instructive comparative analyses of murine hair growth patterns. This guide complements our earlier guide on the classification of murine HF development (Paus *et al*, 1999), which combined provide a standardized method for the analysis of murine HF growth.

Based on fundamental histologic and ultrastructural studies on murine cycling HF (Dry, 1926; Butcher, 1951; Chase *et al*, 1951; Wolbach, 1951; Straile *et al*, 1961; Parakkal, 1969a, b, c, 1970; De Weert *et al*, 1982), we have summarized pragmatic criteria for the recognition of distinct stages of the hair cycle (**Figs 1 and 2**).

This guide suggests basic as well as more advanced auxiliary criteria to define anagen, catagen, and telogen stages of the hair cycle (**Figs 1 and 2**), which are widely applicable to different

Manuscript received May 8, 2000; revised June 1, 2001; accepted for publication March 12, 2001.

Reprint requests to: Dr. Ralf Paus, Department of Dermatology, Universitätsklinikum Hamburg-Eppendorf, Martinistr. 52, D-20246 Hamburg, Germany. Email: paus@ukc.uni-hamburg.de

Abbreviations: a.d., after depilation; AP, alkaline phosphatase; APM, arrector pili muscle; CTS, connective tissue sheath; DP, dermal papilla; ES, epithelial strand; HF, hair follicle(s); HS, hair shaft; NCAM, neural cell-adhesion molecule; SG, sebaceous gland.

0022-202X/01/$15.00 · Copyright © 2001 by The Society for Investigative Dermatology, Inc.

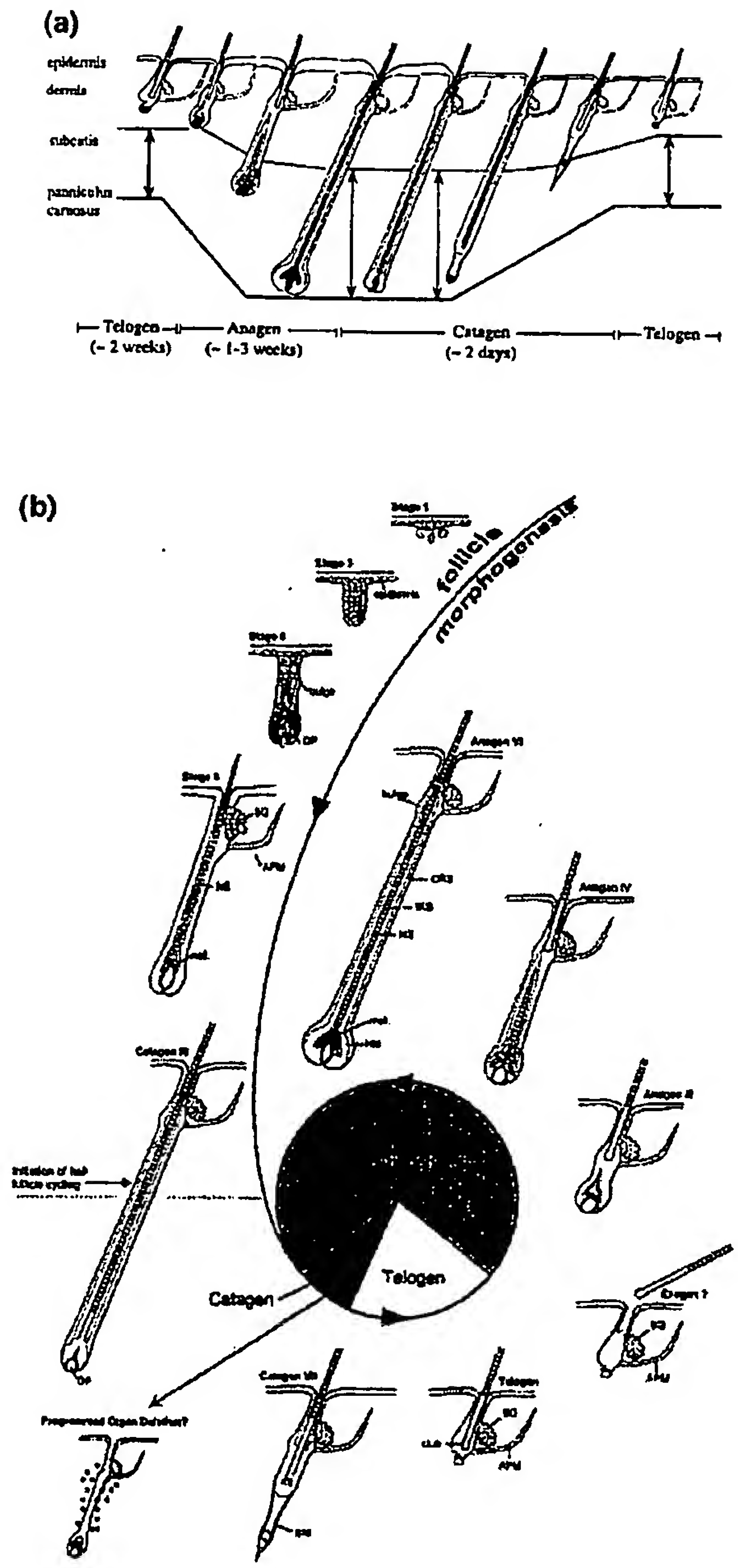

Figure 1. (*a*) Schematic representation of the increasing and decreasing length of the HF and the localization of the most proximal part of the HF in correlation with the panniculus carnosus and the border between the dermis and subcutis. Arrows between panniculus carnosus and the border dermis/subcutis indicate the hair cycle-associated changes in the thickness of the subcutis. The approximate duration of each phase is indicated in brackets. Note changes of the DP shape and size throughout the cycle as well as the increasing size of the SG during anagen IV–VI. (*b*) Schematic representation of key stages of HF development and cycling. Stages 1–8 represent stages of HF development. Anagen: growth phase, catagen: regression phase, telogen: "resting" phase, exogen: (speculative) active shedding phase. For detailed description of programmed organ deletion see Eichmüller *et al*, 1998, for exogen see Stenn and Paus, 2001; black dots refer to immune cells. APM, arrector pili muscle; BM, basement membrane; DP, dermal papilla; HS, hair shaft; IRS, inner root sheath; mel, melanin; ORS, outer root sheath; SG, sebaceous gland.

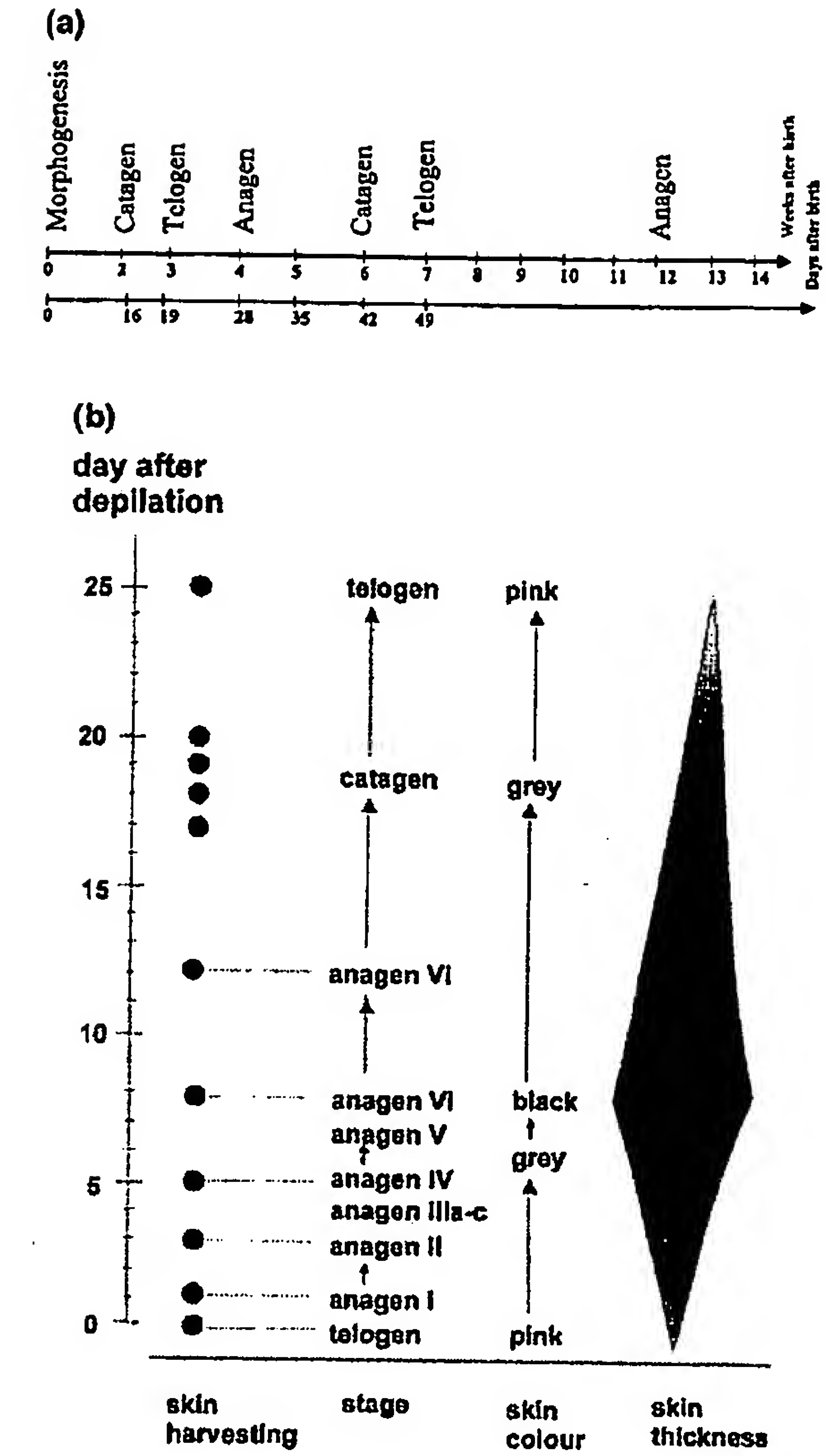

Figure 2. (*a*) Time-scale for the hair cycle in female C57BL/6 mice during the first 14 wk after birth. (*b*) Time-scale for the hair cycle in female C57BL/6 mice and changes of skin pigmentation and skin thickness after depilation.

mouse strains and mutants. In essence, this classification guide can also be utilized for staging the HF of other hairy animals, even though species-specific anatomic differences must be taken into account. The staging guide for mice is also highly relevant for human hair biology, as the same basic follicle transformations occur in mice and men (Kligman, 1959). Until a rigorous comparison of the more subtle morphologic characteristics of murine and human HF cycling has been published, however, it is wise not to claim that the current guide can be used uncritically for human HF staging as well.

HF morphogenesis as well as the first postnatal catagen, telogen, and anagen development follow a rather precise time-scale (Paus *et al*, 1999) (Fig 2*a*). Nevertheless, these processes are dependent on the genetic background (mouse strain), the sex (e.g., female mice show a prolonged telogen) as well as environmental factors such as time of the year (temperature, light periods) and nutritional factors. To avoid associated fluctuations, this current guide is based

on the highly standardized C57BL/6NCrlBR (C57BL/6) model of depilation-induced HF cycling (**Fig 2*b***) (Chase, 1954; Paus *et al*, 1990, 1994a, b). Briefly, a wax/rosin mixture is applied on the dorsal skin of 7 wk old mice with all dorsal skin HF in telogen, as evidenced by the homogeneous pink skin color. Removing the wax/rosin mixture removes all hair shafts and immediately induces homogeneous anagen development over the entire depilated back of the mouse. After full anagen development, the consecutive stages (catagen and telogen) are then entered spontaneously in a fairly homogeneous manner. Compared with spontaneous anagen development, there are two major differences: (i) depilation-induced anagen is fully synchronized over the entire area of depilation, whereas spontaneous anagen develops in a wave-like pattern, and (ii) a slight inflammatory effect of plucking ("wounding response") has been demonstrated (Argyris, 1968), which can also be appreciated by upregulation of epidermal intercellular adhesion molecule-1 immunoreactivity 1 d after depilation (Müller-Röver *et al*, 2000a). Similar to spontaneous anagen, even anagen induced by cyclosporine A, a potent immunosuppressant drug, does not show significant morphological differences compared with depilation-induced hair cycling (Paus *et al*, 1998). No significant differences in the expression patterns of interleukin (IL) -1RI, transforming growth factor (TGF) -βRII or neural cell-adhesion molecule (NCAM) have been found in these three different models (Paus and Müller-Röver, unpublished observation).

Owing to the strict coupling of follicular melanogenesis and HF cycling, anagen development is associated with characteristic changes in skin pigmentation (**Fig 2*b***) (Slominski *et al*, 1991, 1994; Slominski and Paus, 1993). In addition, synchronized HF cycling in mice induces profound alterations in the architecture and thickness of almost all skin compartments, which are most evident in substantial, hair cycle-associated fluctuations in skin thickness (**Fig 2*b***) (Chase, 1954; Paus *et al*, 1990, 1991). Nine days after depilation, the induced anagen HF reach their maximal length and are morphologically indistinguishable from spontaneously developing anagen follicles, even though the plucking trauma induces a short wound healing response immediately after the depilation (Chase *et al*, 1951; Silver *et al*, 1969; Slominski *et al*, 1991; Paus *et al*, 1998). In contrast to the normal caudal-nuchal development of a spontaneously developing anagen wave, spontaneous catagen development starts in the neck region and proceeds in a nuchal-caudal direction. In C57BL/6NCrlBR mice, catagen-associated changes in HF morphology are first seen on day 17 after depilation in the neck region, and are macroscopically recognizable by a switch in skin color from black to gray-pink. The catagen wave reaches the tail region about 2 d later on day 19/20 (Chase *et al*, 1951; Chase, 1954; Straile *et al*, 1961) (**Fig 2**).

HOW TO USE THIS GUIDE

Although spontaneous HF cycling is envisioned to begin with catagen (Paus and Cotsarelis, 1999; Stenn, 1999; Stenn and Paus, 2001) (**Fig 2*a***), hair cycle studies customarily begin with the telogen–anagen transformation. This is reflected in the current guide (**Fig 3**). In order to avoid terminologic confusion, which is often caused by differences in how selected terms are used in hair research papers, we have summarized definitions of key terms employed in the context of this guide (**Table I**). Please note that the term "proximal" here refers to those parts of the HF that are located close to the panniculus carnosus, whereas "distal" refers to those parts located close to the epidermis. In order to illustrate key parameters for the recognition of distinct HF stages throughout the hair cycle, **Fig 3** is structured as follows: the left-hand column shows computer-generated schematic drawings of six distinct main stages and three substages of HF growth (anagen), eight stages of HF regression (catagen) and the quiescence stage (telogen) of the hair cycle, modified from previous works (Chase *et al*, 1951; Straile *et al*, 1961; Paus *et al*, 1997) (for explanation and definition of the corresponding terminology, see **Table I**). The criteria presented here are highly reproducible and reliable in all C57/BL6 mice over a very wide age range, which have been investigated in our group during the last 10 y. These criteria have been described in most pigmented mouse strains, albino mice, and in some mouse mutants (Dry, 1926; Chase *et al*, 1951; Chase, 1954; Orwin *et al*, 1967; Sundberg, 1994; Panteleyev *et al*, 1998, 1999) and are valid also in later cycles of 1 y old mice (Paus and Müller-Röver, unpublished observation).

The central column in **Fig 3** provides a list of basic and auxiliary classification criteria that are separated from each other by a dotted line (top: basic, bottom: auxiliary criteria). The former are recognizable by routine light microscopy, whereas the latter require additional staining methods. The basic criteria are applicable to all mouse strains and are not dependent on the presence of

Telogen

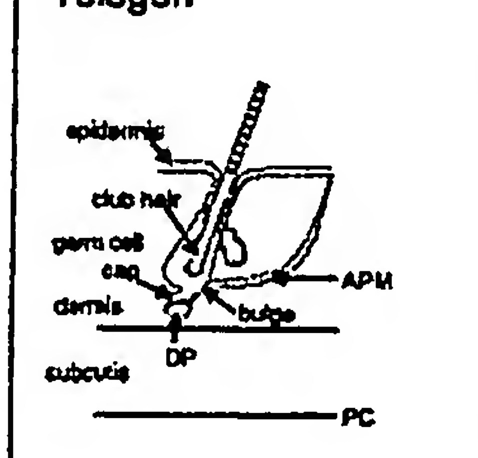

a) entire HF resides in the dermis
b) no IRS
c) compact ball-shaped DP attached to the germ cell cap

d) AP⁺ DP in the dermis
e) IL 1-RI⁺ keratinocytes in the germ capsule, germ cell cap and ORS

Figure 3. A comprehensive guide for the recognition and classification of distinct stages of hair cycling. The left-hand column shows a computer-generated schematic drawing of the so-called quiescence phase (telogen) of the hair cycle. The second column summarizes essential basic criteria for recognition of the single substages (above dotted line) and auxiliary criteria for more precise staging (below dotted line). The right-hand column shows representative micrographs of each hair cycle stage (lower case letters correspond to lower case letters used in the central column). The following staining techniques were employed: (*A*, *C*) Giemsa (Romeis, 1991); (*B*) IL-1 RI immunoreactivity. (Eichmüller *et al*, 1998). *Scale bars*: 50 μm. Please note: upper case letters in the left-hand corner label the image whereas lower case letters identify tissues corresponding to the lower case letters of the criteria listed in the central column. Please also note: the left-hand column lists comprehensively all helpful markers, although not all markers are shown in the micrographs.

Table I. Glossary of anatomical terms frequently used in hair research[a]

Term	Definition
Bulb	Prominent, onion-shaped thickening on the proximal end of the HF; consists of relatively undifferentiated matrix cells, HF melanocytes and of cells from the proximal ORS
Bulge	Convex extension of the distal part of the ORS, near the epidermis, location of epithelial follicle stem cells and point of insertion of the *m.* arrector pili.
Club hair	Resting hair shaft with a hollow brush of keratinized keratinocytes on the proximal end, tightly attached to the cortical cells of the hair cortex
Connective tissue sheath (CTS)	Part of the dermal connective tissue, tightly attached to the outer side of HF, composed of fibroblasts (and macrophages) and connective tissue
Dermal papilla (DP) syn: follicular papilla (FP)	Mesodermal part of the HF, which consists of closely packed mesenchymal cells; framed by the bulb matrix during anagen
Epithelial strand (ES)	Column of epithelial cells between the germ capsule and the compact DP; laterally demarcated by the thickened glassy membrane
Secondary germ capsule syn: secondary hair germ	Bag-like structure of glycogen-free cells (germ cells) of distal ORS, surrounding the club hair
Hair shaft	The hair *per se*, composed of trichocytes (= terminally differentiated HF keratinocytes), divided into hair cuticle, cortex and medulla
Hair shaft medulla	Central part of the hair shaft, composed of large, loosely connected keratinized cells with large intercellular air spaces
Hair shaft cortex	The mass of the hair shaft, composed of keratinized cells, longitudinally packed with keratin filaments (and melanin granules in pigmented hair shafts)
Hair canal	Passage way between epidermal surface and the most distal part of the IRS, demarcated by surrounding ORS.
Hyaline membrane syn: vitreous membrane, glassy membrane	Outermost noncellular part of the HF; composed of basal lamina and two layers of orthogonally arranged collagen fibers; separates ORS from CTS
Infundibulum	Most distal part of the HF in the dermis extending from sebaceous duct to the epidermal surface (including hair canal and distal ORS)
Isthmus	Middle portion of the HF extending from the sebaceous duct to the insertion of the m. arrector pili (bulge region)
Inner root sheath	Multilayered structure composed of terminally differentiated HF keratinocytes surrounded by the ORS; consists of Henle's layer, Huxley's layer and cuticle; surrounds the hair shaft up to the hair canal(IRS)
Outer root sheath (ORS)	Outermost sheath of HF keratinocytes, which merges distally into the basal layer of the epidermis and proximally into the hair bulb
Papillary stock syn: papillary stalk	Fibroblasts that link the proximal pole of the DP and the perifollicular CTS
Sebaceous gland	Glandular structure close to the insertion of the *m. arrector pili* with holocrine function; composed of lipid-filled sebocytes with a foamy appearance

[a]For introductory references, see Chase *et al* (1951); Wolbach (1951); Montagna and Ellis (1958); Montagna and van Scott (1958); Straile *et al* (1961); Roth (1965); Parakkal (1969a); Parakkal (1969c, b, 1970); De Weert *et al* (1982); Cotsarelis *et al* (1990); Abell (1994); Paus *et al*, 1994b; Paus *et al* (1998); Paus and Cotsarelis (1999); Stenn and Paus, 2001.

Table II. Synopsis of auxiliary methods used in this guide[a]

Auxiliary methods/markers	Compartment	Stage	Reference
Pigmented mouse strain			
Melanin granules	Keratogenic region	Anagen IIIa–catagen III	Slominski *et al* (1991, 1994); Slominski and Paus (1993)
Histochemistry			
AP staining	DP	All stages	Handjiski *et al* (1994)
Oil-red-O staining	Sebocytes and hair canal	Anagen IIIc–V	Romeis (1991)
TUNEL staining	hair matrix, ORS, IRS	Catagen I–IV	Lindner *et al* (1997)
Immunohistochemistry			
IL-1 RI	ORS (in contrast to IRS)	All stages	Eichmüller *et al* (1998)
TGF-β RII	ORS (in contrast to IRS)	All stages	Paus *et al* (1997)
NCAM	DP, perifollicular CTS and CTS tail	Catagen IV–VIII	Müller-Röver *et al* (1998)
P-cadherin	Papillary cap, inner hair matrix	Telogen–anagen II	Müller-Röver *et al* (1999)

[a]These methods provide additional help to determine the stage-specific morphology of distinct HF compartments such as the DP or the papillary cap. Additionally, key stages are listed where these methods are of particular value in difficult cases.

pigment granules (melanin) in the HF. The auxiliary criteria that require a pigmented mouse strain such as C57BL/6J, and/or enzyme histochemical techniques, i.e., alkaline phosphatase (AP) and TUNEL staining; or immunohistochemistry for cytokine receptors, such as IL-1 receptor type I (IL-1 RI) and TGF-β receptor type II (TGF-β RII) and adhesion receptors, e.g. NCAM (Table II). The right-hand column in Fig 3 illustrates the criteria listed in the central column with three representative micrographs. The lower case letters used for indicating key parameters correspond to the lower case letters in the central column list. Note that not all parameters are necessarily shown in the right-hand columns.

It is of important to note that the markers used in this guide are by no means the only useful markers for HF staging. For example, staining for soft and hard keratins likely is of great help for the

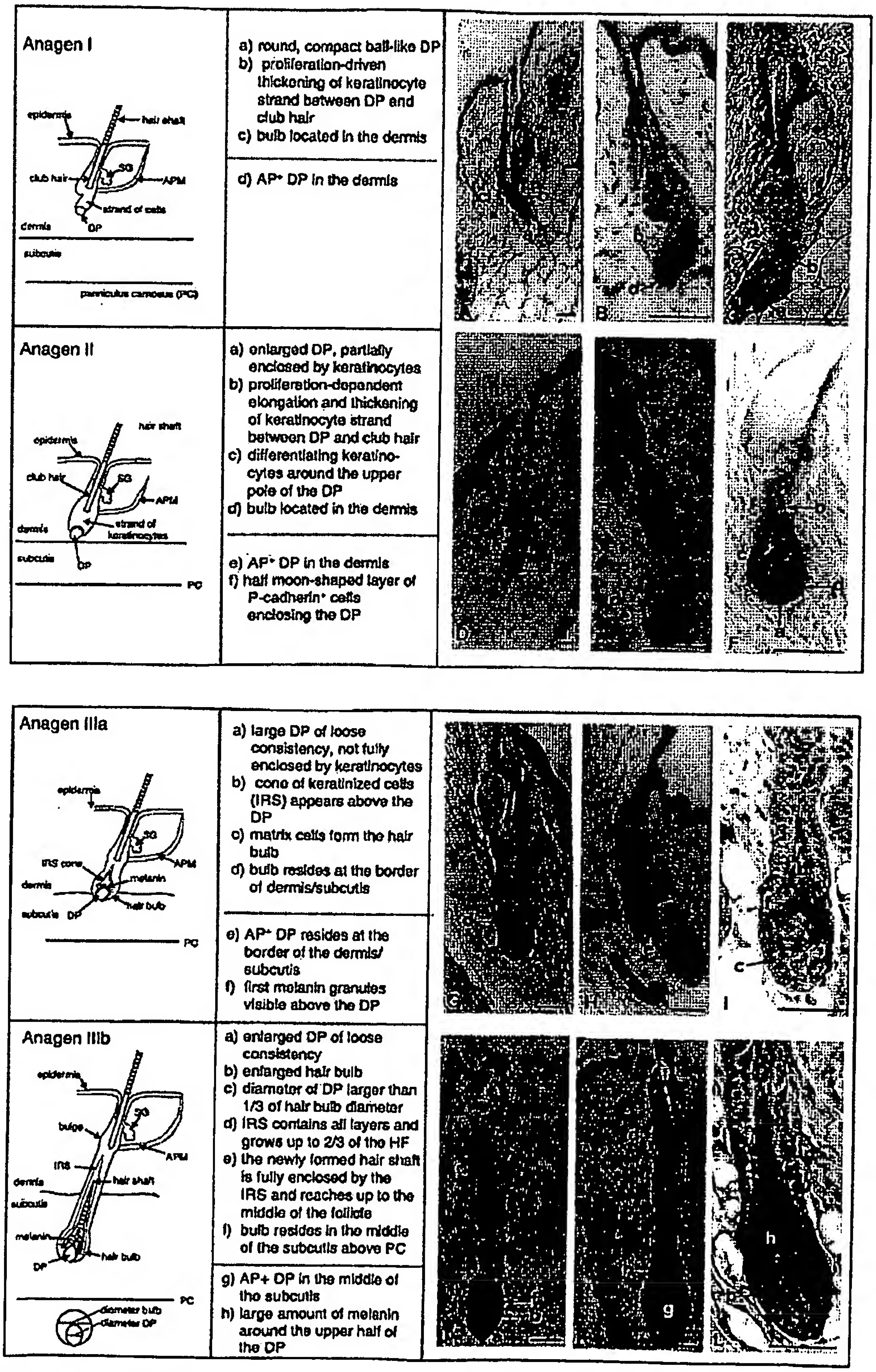

Figure 4. Legend on page 9.

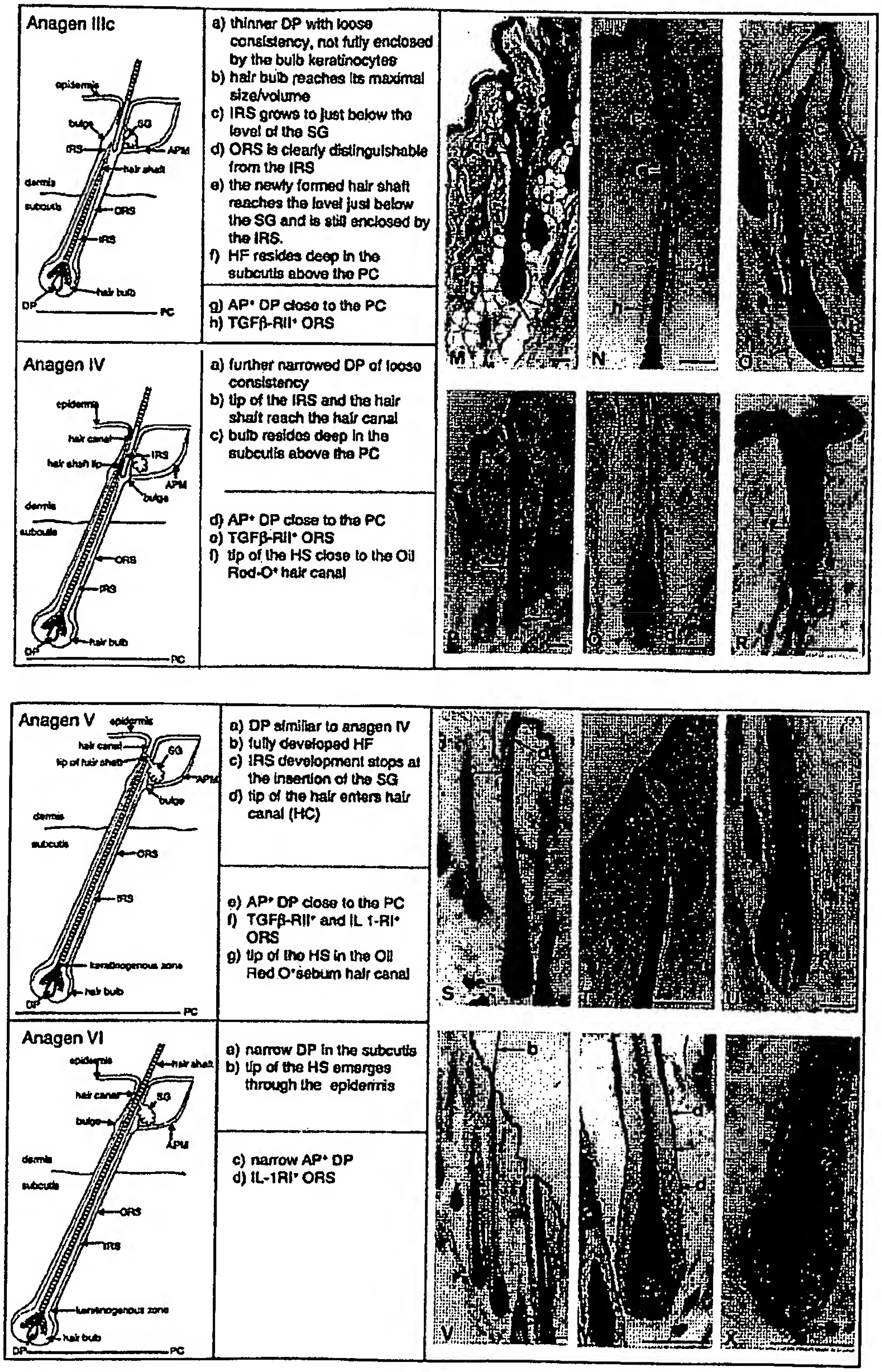

Figure 4. Continued.

recognition and accurate classification of murine HF in different hair cycle stages. Unfortunately, most anti-mouse keratin antibodies we have tested so far show massive background staining, and considerable variations of staining patterns are seen in specific anatomical compartments of the HF at distinct hair cycle stages (Müller-Röver and Paus, unpublished observation). Therefore, we have decided to use antibodies against IL-1R1, TGF-βRII, and NCAM for staining purposes, as these markers show very reliable, highly reproducible follicular staining patterns in specific anatomical compartments throughout hair cycling and experimental hair cycle modulations. Nevertheless, one always needs to consider whether pharmacologic or genetic manipulations in the animals that are to be analyzed might have changed the expression patterns of these markers independently of hair growth and regression (for example: NCAM upregulation in Msx-2 overexpressing mice, Jiang *et al*, 1999).

CRITERIA FOR THE RECOGNITION OF DISTINCT HAIR CYCLE STAGES

Stage-dependent HF length and skin thickness One of the first and easiest parameters used to classify the stage of a HF is its length (Fig 1*b*), which is measured from the dermal papilla (DP) to the epidermis. Anagen I–VI development (Fig 4) is characterized by increasing length of the HF and catagen I–VII by decreasing length (Fig 5). The HF reaches its maximal length during anagen VI (Fig 4*V–X*) and keeps its length during catagen I and II (Fig 5*A–F*). Thus, during anagen VI to catagen II, the DP is located close to the panniculus carnosus. During telogen, the HF reaches its minimal length (Fig 3). Because dermal fibroblasts surround the entire HF during anagens I and II (Fig 4*A–F*) it is strongly advised to use the AP staining method to visualize the DP. Easy to perform, the AP staining method takes only a few minutes, and prevents very common errors during HF staging such as mistaking the epithelial cells of the secondary hair germ of telogen or late catagen HF for fibroblasts of the DP.

As summarized in Figs 1(*b*) and 2(*b*), synchronized HF cycling in mice is also associated with stage-dependent changes of skin thickness and pigmentation. These independent parameters can be utilized to double-check the histomorphometric classification illustrated in Figs 3–5.

Basic rules for the recognition of telogen and anagen I and II HF A HF is in telogen, anagen I or anagen II as long as it is entirely surrounded by dermal fibroblasts and has not yet reached the subcutis. In addition, in pigmented mice, no melanin is visible in the hair matrix above the DP, although occasionally some melanin granules from the preceding anagen phase can be observed in the DP, where they sometimes accumulate (rather than being extruded together with the hair shaft).

Stage-specific characteristics of telogen and anagen I and II HF Telogen HF (Fig 3 *part I A–C*) are very easy to recognize as they are fully surrounded by interfollicular dermal fibroblasts (Fig 3*B*). They do not display any part of the inner root sheath (IRS) and the compact ball-shaped DP is closely attached to a small cap of secondary hair germ keratinocytes (Fig 3*A*, *B*). To distinguish DP and secondary hair germ, either the DP should be visualized by the AP staining method (Fig 3*A*) or the secondary hair germ at the upper pole of the DP should be marked by IL-1 RI immunoreactivity (Fig 3*B*) or P-cadherin immunoreactivity (Müller-Röver *et al*, 1999). In case the morphologic criteria described above are insufficient to distinguish telogen HF and late catagen HF, NCAM immunoreactivity can be employed as a key marker for making this distinction as NCAM immunoreactivity does not reveal more than one or two single NCAM$^+$ connective tissue sheath (CTS) cells in close vicinity to the DP of telogen HF (not shown) whereas late catagen HF display a long tail of trailing NCAM$^+$ CTS fibroblasts (Müller-Röver *et al*, 1998). The number of club hairs in the hair canal is not a reliable parameter for HF staging. In late anagen at least two hair shafts fill the hair canal, the resting shaft from the preceding cycle and the new anagen VI hair shaft. At the end of telogen, some hair shafts are actively shed in a process termed exogen (Stenn *et al*, 1998), whereas others may remain in the hair canal (Fig 4*B*). So far, no telogen substages have been proposed in the literature, but it is still controversially discussed whether the telogen phase is one homogeneous phase of resting (see Stenn *et al*, 1998; Stenn and Paus, 2001).

Similar to telogen HF, anagen I HF (Fig 4*A–C*) are fully enclosed by the dermis. The only obvious difference to telogen HF (see below) is a thickening and prolongation of the strand of keratinocytes between the DP and the club hair. In contrast to anagen II HF, this keratinocyte strand has a smaller diameter than the secondary hair germ of the club hair. In difficult cases, P-cadherin staining is a helpful auxiliary method to visualize specifically the elongating strand of keratinocytes that cap the upper third of the round, compact ball-like DP (Müller-Röver *et al*, 1999).

In contrast, anagen II HF (Fig 4*D–F*) are characterized by an enlarged DP compared with telogen or anagen I HF, which is more than half enclosed by proliferating keratinocytes of the developing hair matrix. The strand of keratinocytes between the DP and the old club hair, i.e., the developing hair bulb, now has a larger

◄

Figure 4. A comprehensive guide for the recognition and classification of distinct stages of hair cycling. The left-hand column shows a computer-generated schematic drawing of the six distinct substages of hair growth (anagen) as suggested by Chase *et al* (1951). The second column summarizes essential basic criteria for recognition of the single substages (above dotted line) and auxiliary criteria for more precise staging (below dotted line). The right-hand column shows representative micrographs of each hair cycle stage (lower case letters correspond to lower case letters used in the central column). The following staining techniques were employed: (*A, C, D, F, G, J, M, O, T, U*) Giemsa (Romeis, 1991); (*W*) IL-1 RI immunoreactivity (Eichmüller *et al*, 1998); (*B, E, H, K, Q, S, V, X*) AP staining (Handjiski *et al*, 1994); (*I, L, M*) periodic acid-Schiff reaction (Romeis, 1991); (*N, P*) TGF-β RII immunoreactivity (Paus *et al*, 1997); (*R*) Oil-Red-O labeling (Romeis, 1991). *Scale bars*: 50 µm. Please note: upper case letters in the left-hand corner label the image whereas lower case letters identify tissues corresponding to the lower case letters of the criteria listed in the central column. Please also note: the left hand column lists comprehensively all helpful markers, although not all markers are shown in the micrographs.

►

Figure 5. A comprehensive guide for the recognition and classification of distinct stages of hair cycling. The left-hand column shows a computer-generated schematic drawing of the eight distinct stages of HF regression (catagen) as suggested by Straile *et al* (1961). The second column summarizes essential basic criteria for recognition of the single substages (above dotted line) and auxiliary criteria for more precise staging (below dotted line). The right-hand column shows representative micrographs of each hair cycle stage (lower case letters correspond to lower case letters used in the central column). The following staining techniques were employed: (*A, B, D, E, H, K, M, P, S, U, V, X*) Giemsa (Romeis, 1991); (*C, G, I, J, N, Q, T*) AP staining (Handjiski *et al*, 1994); (*F, L*) TUNEL (Lindner *et al*, 1997); (*O, R, W*) NCAM immunoreactivity (Müller-Röver *et al*, 1998). *Scale bars*: 50 µm. Please note: upper case letters in the left-hand corner label the image whereas lower case letters identify tissues corresponding to the lower case letters of the criteria listed in the central column. Please also note: the left-hand column lists comprehensively all helpful markers, although not all markers are shown in the micrographs.

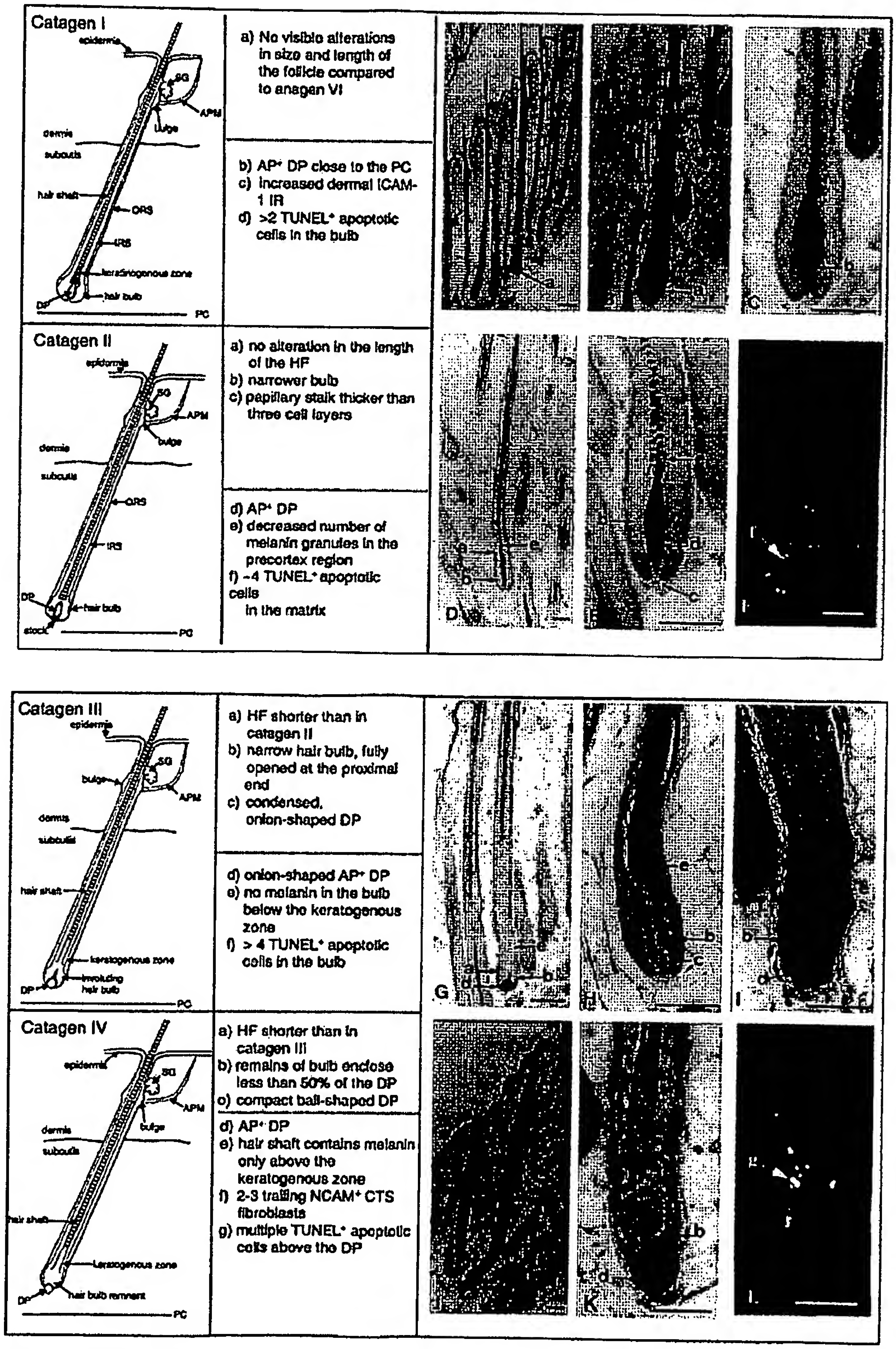

Figure 5. Legend on page 9.

Catagen V

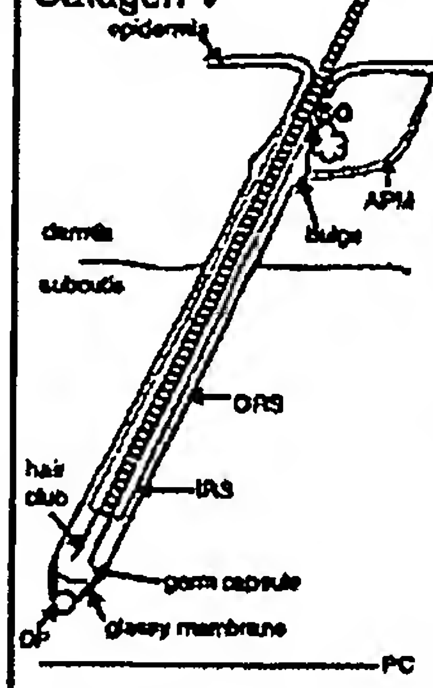

a) HF shorter than in catagen IV
b) compact ball-shaped DP
c) development of club hair
d) ORS forms the germ capsule around the club hair
e) regression of IRS with sharply demarcated borders
f) epithelial constriction between germ capsule and DP
g) thick glassy membrane around the constricted part of the HF
h) apoptotic cells in the constricted part of the HF

i) AP+ DP
j) length of trailing NCAM+ CTS = DP diameter

Catagen VI

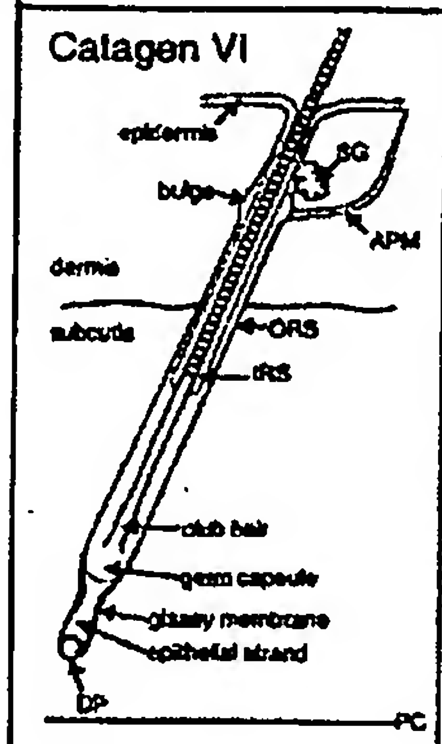

a) brush-like club moves distally
b) compact ball-shaped DP remains in the subcutis
c) epithelial strand (ES) between DP and germ capsule longer than diameter of DP
d) very thick glassy membrane surrounds the ES
e) multiple apoptotic cells in ES
f) very sharply demarcated IRS borders

g) AP+ DP in the subcutis
h) length of trailing NCAM+ CTS = DP diameter

Catagen VII

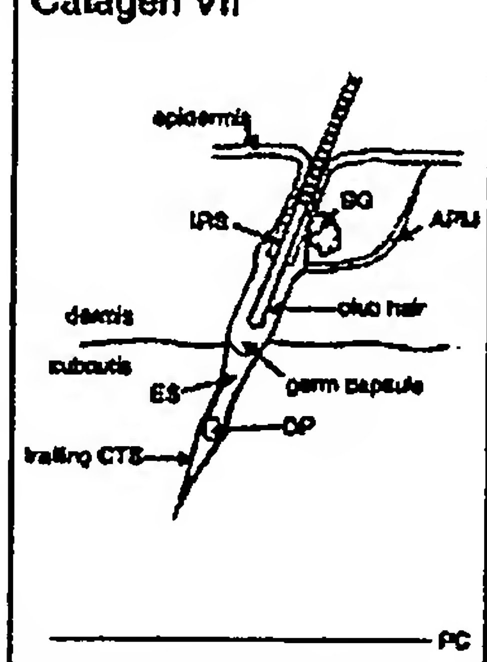

a) fully keratinized hair-club and germ capsule at the border dermis/subcutis
b) epithelial strand (ES) longer than DP diameter
c) prominent trailing CTS
d) apoptotic cells in the ES

e) AP+ DP with trailing CTS in the subcutis
f) trailing NCAM+ CTS >2 times longer than DP diameter

Catagen VIII

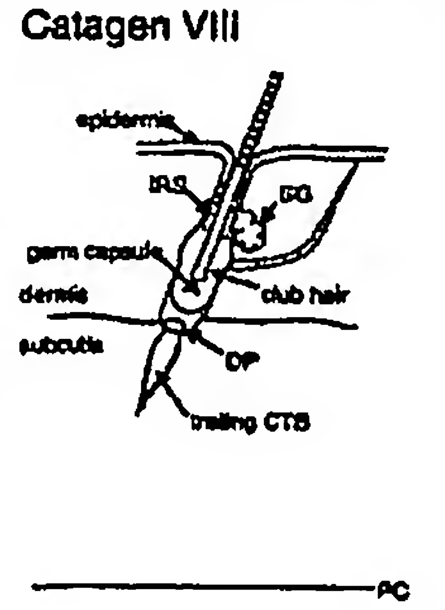

a) germ capsule and club hair in the dermis
b) DP at the border dermis/subcutis
c) trailing CTS with folded glassy membrane in subcutis
d) remnants of IRS at the level of the SG

e) AP+ DP at the border dermis/subcutis
f) trailing NCAM+ CTS >3 times longer than DP diameter

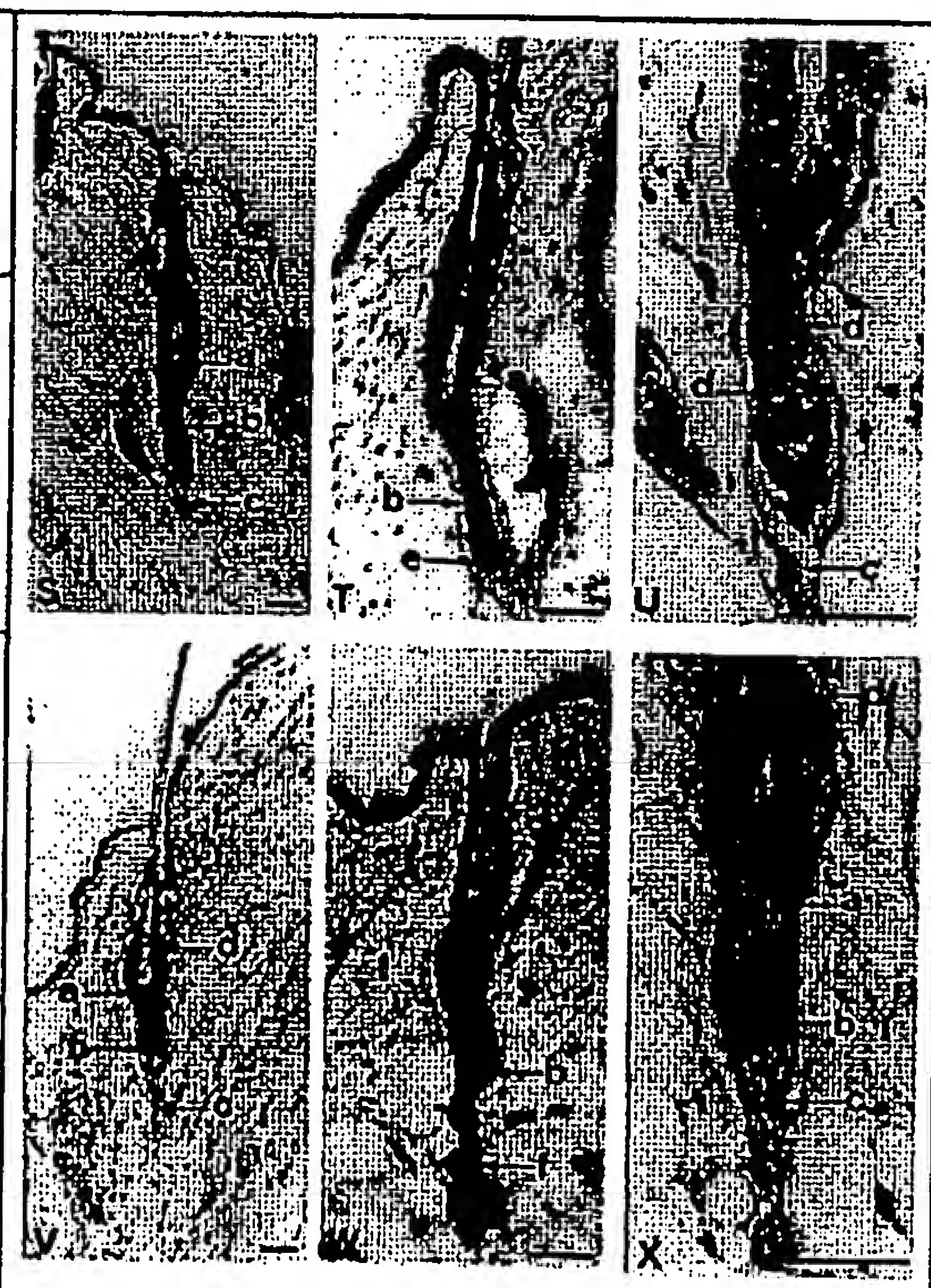

Figure 5. Continued.

diameter than the secondary hair germ of anagen I HF. The developing bulb and the DP are located at the border between the dermis and the subcutis. The upper pole of the DP of an anagen HF is surrounded by a half moon-shaped layer of keratinocytes that display a corona-like orientation, which one can easily visualize by P-cadherin immunoreactivity (Müller-Röver *et al*, 1999).

Anagen III: proposal to distinguish three distinct substages One aim of this guide is to standardize the description of hair cycle-dependent gene and protein expression patterns. In this context, it is a dilemma that the classical hair research literature (Chase *et al*, 1951; Chase, 1954; Straile *et al*, 1961) divides the hair cycle precisely in 15 different stages with a high descriptive value, whereas from a pragmatic point of view this may appear overdetailed and functionally insignificant. On the one hand, however, only this high degree of distinction allows one to detect even subtle abnormalities in HF cycling that had previously remained unnoticed (e.g., Maurer *et al*, 1997b; Botchkarev *et al*, 1998, 1999). On the other hand, it cannot be overemphasized that even "minor" alterations in follicle morphology from one of the well-defined substages of the hair cycle to the next reflect massive changes in gene expression, cell migration, proliferation, differentiation, apoptosis, and matrix remodeling. It is therefore conceivable that even more substages will have to be defined in the future, once the morphologic signs of cyclic HF transformation have been more rigorously and systematically lined up with the underlying changes in cell biology and gene expression.

The HF is in anagen III when the hair bulb surrounds the DP and resides at the border between dermis and subcutis or deeper, and when the tip of the newly formed IRS is below the hair canal. It is advisable to subdivide the historical stage "anagen III" into three substages for the following reasons. First, anagen III is the second longest phase of the murine hair cycle (approximately 3 d, with only anagen VI lasting longer; see **Fig 2*b***) compared with the relatively short anagen I–II and IV–V phases and this encompasses massive morphologic changes in the follicle, which follow a easily distinguishable choreography of follicle transformation events. Secondly, anagen IIIa is characterized by the onset of melanogenesis (Chase *et al*, 1951; Slominski *et al*, 1994) and the formation of the IRS cone, whereas anagen IIIb and IIIc are characterized by a fully developed IRS and a fully developed, pigmented hair shaft. Thirdly, the follicular DP is located at the border dermis/subcutis (in anagen IIIa), in the middle of the subcutis (in anagen IIIb) or close to the panniculus carnosus (in anagen IIIc). Finally, the bulb reaches its maximal size not before anagen IIIc (Chase *et al*, 1951; Chase, 1954). Each of these distinct processes is a primary target of pharmacologic or genetic manipulation and the effect of a given test agent may well differ between each of these three distinct substages of anagen III. Considering the magnitude of changes on the cell and extracellular matrix level (proliferation, migration, apoptosis, differentiation, melanogenesis, matrix synthesis) that corresponds to each of these anagen III substages, even this additional subdivision, in the future, may still be considered too crude. In the interest of practicability, however, it offers a reasonable compromise between user-friendliness and hair biologic necessities.

Characteristics of anagen IIIa, IIIb, and IIIc HF In anagen IIIa HF (**Fig 4*G–I***) the bulb and DP reside at the border between the dermis and subcutis. During anagen IIIb (**Fig 4*J–L***), the DP and bulb reside in the middle of the subcutis. Finally, during anagen IIIc (**Fig 4*M–O***), the DP and bulb reside close to the panniculus carnosus.

Although in both cases the bulb is located close to the border between dermis and subcutis anagen II and IIIa HF are distinguished by the fact that anagen IIIa HF show the IRS cone above the DP and (in pigmented mice) melanin granules first appear within the developing IRS cone (**Fig 4*G–I***). The developing IRS becomes detectable as a layer of differentiated keratinocytes arising from the most distal hair matrix and is visible as a cone-shaped structure that reaches up to the middle of the developing anagen HF (**Fig 4*I***). No hair shaft is visible at this time, as it forms only after the completion of anagen IIIa.

A developing hair shaft becomes clearly visible in anagen IIIb HF (**Fig 4*J–L***). It reaches up to the middle of the HF, and is entirely surrounded by the IRS, which now contains all three of its layers (Henle's layer, Huxley's layer, cuticle). The distal tip of the IRS reaches up to two-thirds of the length of the HF, but still resides below the level of the old club hair, the insertion of the arrector pili muscle, and the sebaceous gland (SG) (**Fig 4*J–L***). The bulb is now larger than in anagen IIIa, and fully encloses the enlarged DP. The DP now has a looser consistency and it makes up more than one-third of the bulb volume (see small insert diagram on p. 7 below the schematic representation of anagen IIIb). The bulb and DP of anagen IIIb HF reside in the mid-subcutis (**Fig 4*J–L***).

During anagen IIIc (**Fig 4*M–O***), the bulb and DP reach their deepest (i.e., most proximal) position and come to rest close to the panniculus carnosus in the subcutis (**Fig 4*M***). The IRS and the hair shaft now reside just below the level of the SG, but do not reach the hair canal (**Fig 4*N*, *O***). The outer root sheath (ORS) and IRS are clearly distinguishable (**Fig 4*N***). In order to determine the precise location of the IRS tip, TGF-β RII immunoreactivity is a very useful auxiliary parameter because only the ORS is positive for this marker (Paus *et al*, 1997). Compared with anagen IIIb, the DP is now thinner and more elongated, but is still of loose consistency and not yet fully surrounded by hair bulb keratinocytes (**Fig 4*O***).

Basic rule for the differentiation of anagen IIIc to anagen VI/catagen I HF The key technique for distinguishing anagen IIIc, IV, V and VI HF is to assess the exact position of the hair shaft and the IRS: during anagen IIIc, the hair shaft and IRS reach a level just below the insertion of the SG; during anagen IV, both hair shaft and IRS have reached the hair canal; during anagen V, the tip of the newly formed hair shaft enters into the hair canal; and during anagen VI, the tip of the hair shaft (early anagen VI) and beyond (late anagen VI/catagen I) emerge through the pilary canal to the skin surface.

Stage-specific characteristics of anagen IV to anagen VI/catagen I HF During the short anagen IV phase (**Fig 4*P–R***), the bulb and DP still reside in the deep subcutis (**Fig 4*P*, *Q***). Compared with anagen III, the bulb is enlarged and the DP is narrowed, thus, the diameter of the DP is smaller than one-third of the bulb diameter. That the distal end of the IRS and the tip of the hair shaft are closely attached to the hair canal (**Fig 4*R***) serves as the basic parameter to distinguish anagen IV from the previous and consecutive stages. TGF-β RII immunoreactivity in the ORS gives a perfect outline of the TGF-β RII-negative IRS (**Fig 4*P***). In order to determine precisely whether the hair shaft has already entered the hair canal, the Oil-Red-O technique (Romeis, 1991) is particularly helpful as it stains the sebum in the hair canal (**Fig 4*R***).

Similar to the preceding stage, anagen V (**Fig 4*S–U***) is a very short phase. Anagen V HF are easily recognized as at this time the tip of the hair shaft has entered the hair canal and is still fully enclosed by the ORS (**Fig 4*T***). The DP has a similar shape, volume, and appearance as in anagen IV and VI (**Fig 4*S*, *U***). IRS degradation begins at the level of the insertion of the SG (**Fig 4*T***). In difficult cases, Oil Red-O staining helps to reveal the precise position of the tip of the hair shaft in the sebum-filled hair canal (cf. **Fig 4*R***). When the tip of the hair shaft emerges through the epidermis, the HF enters anagen VI (**Fig 4*V***). The narrow, elongated DP and the bulb reside close to the panniculus carnosus.

Anagen VI (**Fig 4*V*, *X***) and catagen I HF **Fig 5*A–C***) cannot be distinguished by light microscopic morphologic criteria. For catagen, we use the TUNEL method to identify apoptotic keratinocytes. Any HF with more than two TUNEL$^+$ cells in the bulb is defined as a catagen I HF, as the rate of TUNEL labeling is closely related to the morphologic changes during catagen development (Weedon and Strutton, 1984; Lindner *et al*, 1997).

Recognition of catagen II–IV HF The basic parameter characterizing catagen II–IV HF are: (i) the shape of the DP [as

it is best visualized by AP histochemistry (Handjiski *et al*, 1994) or NCAM immunohistochemistry (Müller-Röver *et al*, 1998)], and (ii) the shape of the bulb (catagen II HF displays a smaller epithelial bulb, which completely surrounds a long, oval DP; catagen III HF displays an onion-shaped DP that is predominantly, but not completely enclosed by the hair bulb; and catagen IV HF display a compact, ball-shaped DP that is surrounded by the bulb for less than half of its volume).

During catagen II (**Fig 5*D–F***), the follicle retains its anagen VI/catagen I length (**Fig 5*D***), but compared with anagen VI/catagen I HF has a smaller bulb (**Fig 5*D–F***) and a narrower DP (**Fig 5*E*, *F***). In addition, the papillary stock (= papillary stalk) that links the DP and the perifollicular CTS is thickened and now contains more than three cell layers (**Fig 5*F***).

In pigmented HF, as in C57BL/6NCrlBR mice, catagen II is very easy to distinguish as a dramatic reduction of the number of melanin granules is found in the precortical hair matrix (**Fig 5*D*, *E***) (Slominski *et al*, 1994). TUNEL staining, as an auxiliary method, reveals that up to four TUNEL$^+$ keratinocytes are present in the hair bulb (Lindner *et al*, 1997).

Catagen III HF (**Fig 5*G–I***) are visibly shorter than catagen II HF, although the bulb and DP are still located close to the panniculus carnosus (**Fig 5*G***). Although the follicle is shorter, the latter is due to the simultaneously declining overall skin thickness (**Fig 1*a*, 2*b***). The key characteristic of this stage is the onion-like shape of the DP, a feature not found in any other stage (**Fig 5*G*, *I***). At this time the bulb is smaller and encloses no more than half of the DP (**Fig 5*G***). The characteristic onion-like shape of the DP and the open end of the bulb are particularly well visualized by the AP staining method (**Fig 5*G*, *I***). In pigmented HF, no melanin granules are seen in the precortical hair matrix and the keratogenous region (**Fig 5*H*, *I***). The presence of more than four TUNEL$^+$ in the bulb is an auxiliary criterion for recognizing catagen III HF.

As for catagen III in catagen IV (**Fig 5*J–L***) the shortening of the HF is compensated by the substantial, catagen-associated reduction in skin thickness so that the hair bulb and DP remain located close to the panniculus carnosus (**Figs 4*P* and 5*J***). The key parameter for recognizing this stage is the compact, ball-like shape of the DP and the retracted bulb both clearly demarcated by the AP staining method (**Fig 5*K***). In pigmented HF, only the distal part of the hair shaft is still pigmented (**Fig 5*J***). Using NCAM immunoreactivity as an auxiliary marker (Müller-Röver *et al*, 1998), only two to three trailing NCAM$^+$ CTS cells are visible. Numerous TUNEL$^+$ keratinocytes are now present in the bulb.

Recognition of catagen V–VIII HF Catagen V–VI HF (**Fig 5*M–R***) display a characteristic "epithelial strand" between the secondary germ capsule and the DP. Whereas this epithelial strand represents only a small insertion between the DP and germ capsule in catagen V HF, catagen VI and VII HF display an epithelial strand that is substantially longer than the diameter of the DP (**Fig 5*P–U***). Catagen VI–VIII HF can be differentiated by the length of the trailing CTS "tail" proximal to the DP: the trailing CTS tail of catagen VI HF is not longer than the DP diameter (**Fig 5*Q*, *R***), whereas it is twice as long as the DP diameter during catagen VII (**Fig 5*S–U***) and three times as long during catagen VIII (**Fig 5*V*, *X***). Anti-NCAM labeling should be used as an auxiliary method in order to determine the precise length of the trailing NCAM$^+$ CTS tail—one of the major parameters for distinguishing catagen VI, VII, and VIII, and telogen (**Fig 5*R*, *W***) (Müller-Röver *et al*, 1998).

During catagen V, the overall skin thickness as well as the HF length are substantially reduced. Yet, the compact, ball-shaped DP is still located in the subcutis (**Fig 5*M–O***). The key characteristics of this stage are: (i) the development of the club hair, and (ii) the formation of the secondary germ capsule around the proximal end of the developing club hair (**Fig 5*M–O***) leading to a constriction of the developing epithelial strand between the DP and germ capsule. The developing club hair base is characterized as a brush-like structure at the most proximal depigmented end of the hair shaft, which is surrounded by about three cell layers of the developing secondary hair germ (ORS) (**Fig 5*M–O***). Furthermore, the IRS begins to appear more opaque, and displays more sharply demarcated borders (**Fig 5*M***). Using NCAM immunoreactivity as an auxiliary method reveals a trailing "tail" of NCAM$^+$ CTS cells proximal to the DP, which may be as long as the diameter of the DP (**Fig 5*O***).

Catagen VI HF (**Fig 5*P–R***) are characterized by a clearly visible, brush-like hair club base that is entirely surrounded by the germ capsule (ORS) and has started to move distally (**Fig 5*Q***). The opaque IRS is now very sharply demarcated from the ORS (**Fig 5*Q***). The epithelial strand is longer than the diameter of the DP (**Fig 5*R***). It is surrounded by a thick, glassy membrane, and contains multiple apoptotic (i.e., small pyknotic) keratinocytes that are frequently visible. The NCAM$^+$ tail of trailing CTS fibroblasts is not longer than the diameter of the DP (**Fig 5*R***).

The key parameter distinguishing catagen VII HF (**Fig 5*S–U***) from catagen VI is the upward movement of the DP, leaving behind a long tail of CTS fibroblasts (**Fig 5*S–U***). Stenn *et al* (1998) proposed the concept of the "apoptotic force" to explain the upward movement of the DP (cf. Stenn and Paus, 2001): as catagen HF are characterized by an increased rate of apoptotic cell death in the bulb and epithelial strand (Lindner *et al*, 1997) the volume of the proximal HF is increasingly reduced. Because the surviving keratinocytes are still linked by adhesion receptors such as E- and P-cadherin (Müller-Röver *et al*, 1999), the progressively reduced size of the proximal HF moves the attached DP upwards within the CTS. The CTS tail is at least twice as long as the DP diameter (**Fig 5*S–U***). Although the CTS tail is now clearly visible by light microscopy, it is particularly helpful to use anti-NCAM labeling to determine the precise length of the NCAM$^+$ CTS tail, which is now more than twice as long as the DP diameter during catagen VII. The epithelial strand – still at least twice as long as the DP diameter (**Fig 5*S–U***) – displays numerous apoptotic cells (**Fig 5*U***) (Lindner *et al*, 1997). AP labeling helps to locate the DP precisely, which has now moved upwards, resting in the middle of the subcutis (**Fig 5*T***).

Catagen VIII HF (**Fig 5*V–X***) are substantially shorter than catagen VII HF. Now the germ capsule as well as the club hair base reside in the dermis (**Fig 5*V*, *W***). The DP is located at the border between the dermis and subcutis (**Fig 5*V*, *W***). The trailing CTS tail, which consists of the folded glassy membrane as well as some fibroblasts and macrophages, still resides in the subcutis (**Fig 5*V*, *X***). Remnants of the IRS are still present at the level of the SG (**Fig 5*V*, *X***). In order to avoid the common error of mistaking the CTS tail or the secondary hair germ for the DP, it is again very helpful to use the AP staining technique.

Catagen VIII and telogen HF are distinguished by the length of the trailing CTS using NCAM immunoreactivity: the trailing NCAM$^+$ CTS is more than three times longer than the DP diameter in catagen VIII HF (**Fig 5*W***), whereas it is absent in telogen HF.

ANALYSIS OF HAIR CYCLE ALTERATIONS IN MUTANT OR PHARMACOLOGICALLY TREATED MICE

Using the qualitative criteria characterized in this guide, it is possible to provide fully quantitative comparisons of abnormalities in HF cycling in mutant (transgenic, knockout, spontaneous mutants) or pharmacologically treated mice compared with age-matched wild-type or vehicle controls. For quantitative experiments, a sufficiently large number of age- and sex-matched test and control mice should be compared by quantitative histomorphometry, i.e., the morphologic criteria described above should be used to determine the stages of a defined number of longitudinally cut HF per mouse (e.g., 20 HF per mouse, studying three to five mice per time point and group). Quantitative histomorphometry for the study of abnormalities in murine HF cycling, using the classification criteria suggested here, has been used by us in previous

publications (Paus *et al*, 1994b; Maurer *et al*, 1997b, 1998; Schilli *et al*, 1997; Botchkarev *et al*, 1998, 1999; Müller-Röver *et al*, 2000a, b).

For the qualitative and quantitative evaluation of HF it is of pivotal importance to study standardized longitudinal sections of HF, prepared by using a special harvesting and embedding technique (Paus *et al*, 1999). A sufficient number of well-cut skin sections has to be prepared for each mouse in order to assign the HF to defined hair cycle stages. The total number of HF per hair cycle stage (anagen I–VI, catagen I–VIII, telogen) then can be compared quantitatively and statistically between test and control mice.

This quantitative approach can be developed further by calculating a "hair cycle score" as described previously (Maurer *et al*, 1997a, b): This allows one to compare either anagen or catagen development between large cohorts of HF from test and control groups of mice. To this end every stage of anagen or catagen is assigned a factor in ascending numerical order (e.g. for anagen: anagen I = factor 1, anagen II = factor 2, anagen III = factor 3, etc.; for catagen: catagen I = factor 1, catagen II = factor 2, catagen III = factor 3, etc.). The number of HF in each specific stage is multiplied by the corresponding factor. The results of each sum are totalled and divided by the total number of HF counted. This gives a final value between 1 and 6 for anagen HF and between 1 and 8 for catagen HF, thus defining the average stage of all HF within the entire group. This will allow one to identify even subtle abnormalities in the dynamics of HF cycling between test and control mice that might otherwise have escaped notice. In addition, we have to highlight that HF located close to each other very rarely display vastly different stages; therefore, "outlying" HF stages are also very rarely seen. In these rare cases, however, the statistical results have to be interpreted carefully.

More severe alterations of the skin phenotype such as might be caused by a spontaneous or experimentally induced mutation, can result in a large number of alterations to the HF phenotype (Sundberg, 1994), including the induction of HF dystrophy, i.e., morphologic signs of HF damage such as abnormally distended hair canals, massive apoptosis, and ectopic melanin granules (cf. Paus *et al*, 1994c, 1996; Maurer *et al*, 1997b; Schilli *et al*, 1998). A drug effect on hair cycling or the pathogenesis of a mutation can only be understood fully if the exact stage is known when the aberrations are seen for the first time (for a good example see Panteleyev *et al*, 1998). In any case, critical analysis of alterations in the speed and synchronization of HF cycling, and in the morphology of defined HF compartments requires implementation and quantification of such assessment criteria as suggested in this guide.

In summary, this review offers a comprehensive, pragmatic, and simple guide to recognizing the morphologic features of murine HF cycling, and serves as a useful tool for rapid and instructive analyses of mouse hair phenotypes after genetic or pharmacologic manipulations. The schematic drawings of individual hair cycle stages presented here may be employed by other investigators for reporting the follicular expression patterns of their genes and proteins of interest so that the documentation of such expression patterns will provide a framework for a standardized and highly reproducible comparison.

The excellent technical assistance of R. Pliet and E. Hagen, and the most helpful critical suggestions of C. Ling, U. Hofmann and M. P. Philpott are most gratefully acknowledged. This study was supported in part by a grant from the European Union (Brite-Euram 3: BE97-4301) to RP and IAM.

REFERENCES

Abell E: Embryology and anatomy of the hair follicles. In: Olsen EA (ed.). *Disorders of Hair Growth*. New York: McGraw Hill, 1994: pp. 1–20.

Argyris TS: Growth induced by damage. *Adv Morphol* 7:1–43, 1968

Botchkarev V, Welker P, Albers K, *et al*: A new role for neurotrophin-3: involvement in the regulation of hair follicle regression (catagen). *Am J Pathol* 153:279–285, 1998

Botchkarev VA, Botchkareva NV, Welker P, *et al*: A new role for neurotrophins: involvement of brain-derived neurotrophic factor and neurotrophin-4 in hair cycle control. *FASEB J* 13:395–410, 1999

Butcher EO: Development of the pilary system and the replacement of hair in mammals. *Ann N Y Acad Sci* 53:508–515, 1951

Chase H: Growth of the hair. *Physiol Rev* 113–126, 1954

Chase HB, Rauch H, Smith VW: Critical stages of hair development and pigmentation in the mouse. *Physiol Zool* 24:1–9, 1951

Cotsarelis G, Sun TT, Lavker RM: Label-retaining cells reside in the bulge area of pilosebaceous unit: implications for follicular stem cells, hair cycle, and skin carcinogenesis. *Cell* 61:1329–1337, 1990

De Weert J, Kint A, Geerts ML: Morphological changes in the proximal area of the rat's hair follicle during early catagen. An electron-microscopic study. *Arch Dermatol Res* 272:79–92, 1982

Dry E: The coat of the mouse (*Mus musculus*). *J Genet* 287–340, 1926

Eichmüller S, van der Veen C, Moll I, Hermes B, Hofmann U, Müller-Röver S, Paus R: Clusters of perifollicular macrophages in normal murine skin: physiological degeneration of selected hair follicles by programmed organ deletion. *J Histochem Cytochem* 46(3):361–370, 1998

Handjiski B, Eichmüller S, Hofmann U, Czarnetzki BM, Paus R: Alkaline phosphatase activity and localization during the murine hair cycle. *Br J Dermatol* 131:303–310, 1994

Jiang TX, Liu YH, Widelitz RB, Kundu RK, Maxson RE, Chuong CM: Epidermal dysplasia and abnormal hair follicles in transgenic mice overexpressing homeobox gene MSX-2. *J Invest Dermatol* 113(2):230–237, 1999

Kligman AM: The human hair cycle. *J Invest Dermatol* 33:307–316, 1959

Lindner G, Botchkarev VA, Botchkarev NV, Ling G, van der Veen C, Paus R: Analysis of apoptosis during murine hair follicle regression (catagen). *Am J Pathol* 151(6):1601–1617, 1997

Maurer M, Fische E, Handjiski B, Barandi A, Meingasser J, Paus R: Activated skin mast cells are involved in hair follicle regression (catagen). *Lab Invest* 319–332, 1997a

Maurer M, Handjiski B, Paus R: Hair growth modulation by topical immunophilin ligands: Induction of anagen, inhibition of massive catagen development, and relative protection from chemotherapy-induced alopecia. *Am J Pathol* 150:1433–1441, 1997b

Maurer M, Peters EM, Botchkarev VA, Paus R: Intact hair follicle innervation is not essential for anagen induction and development. *Arch Dermatol Res* 290:574–578, 1998

Montagna W, Ellis RA: *The Biology of Hair Growth*. New York: Academic Press, 1958

Montagna W, van Scott EJ: The anatomy of the hair follicle. In: Montagna W, van Scott EJ (eds). *The Biology of the Hair Growth*. New York: Acadenic Press, 1958: pp. 56–65.

Müller-Röver S, Peters EJM, Botchkarev VA, Panteleyev A, Paus R: Distinct patterns of NCAM expression are associated with defined stages of murine hair follicle morphogenesis and regression. *J Histochem Cytochem* 46:1401–1410, 1998

Müller-Röver S, Tokura Y, Welker P, Furukawa F, Wakita H, Takigawa M, Paus R: E- and P-cadherin expression during murine hair follicle development and cycling. *Exp Dermatol* 8:237–246, 1999

Müller-Röver S, Bulfone-Paus S, Handjiski B, *et al*: ICAM-1 and hair follicle regression. *J Histochem Cytochem* 48:557–568, 2000a

Müller-Röver S, Rossiter H, Paus R, *et al*: Overexpression of bcl-2 protects from UVB-induced apoptosis, but promotes hair follicle regression and chemotherapy-induced alopecia. *Am J Pathol* 156:1395–1405, 2000b

Orwin DF, Chase HB, Silver AF: Catagen in the hairless house mouse. *Am J Anat* 121:489–508, 1967

Panteleyev AA, van der Veen C, Rosenbach T, Müller-Röver S, Sokolov VE, Paus R: Towards defining the pathogenesis of the hairless phenotype. *J Invest Dermatol* 110:902–907, 1998

Panteleyev AA, Botchkareva NV, Sundberg JP, Christiano AM, Paus R: The role of the hairless (hr) gene in the regulation of hair follicle catagen transformation. *Am J Pathol* 155:159–171, 1999

Parakkal PF: The fine structure of anagen hair follicle of the mouse. In: Montagna W, Dobson RL (eds). *Advances in Biology of Skin*. Oxford: Pergamon Press, 1969a

Parakkal PF: Role of macrophages in collagen resorption during hair growth cycle. *J Ultrastruct Res* 29:210–217, 1969b

Parakkal PF: Ultrastructural changes of the basal lamina during the hair growth cycle. *J Cell Biol* 40:561–564, 1969c

Parakkal PF: Morphogenesis of the hair follicle during catagen. *Z Zellforsch Mikrosk Anat* 107:174–186, 1970

Paus R: Control of the hair cycle and hair diseases as cycling disorders. *Curr Opin Dermatol* 3:248–258, 1996

Paus R: Principles of hair cycle control. *J Dermatol (Tokyo)* 25:793–802, 1998

Paus R, Cotsarelis G: Biology of the hair follicle. *N Engl J Med* 341:491–497, 1999

Paus R, Stenn KS, Link RE: Telogen skin contains an inhibitor of hair growth. *Br J Dermatol* 122:777–784, 1990

Paus R, Stenn KS, Elgjo K: The epidermal pentapeptide pyroGlu-Glu-Asp-Ser-GlyOH inhibits murine hair growth in vivo and in vitro. *Dermatologica* 183:173–178, 1991

Paus R, Eichmüller S, Hofmann U, Czarnetzki BM: Expression of classical and non-classical MHC class I antigens in murine hair follicles. *Br J Dermatol* 131:177–183, 1994a

Paus R, Handjiski B, Czarnetzki BM, Eichmüller S: A murine model for inducing and manipulating hair follicle regression (catagen): effects of dexamethasone and cyclosporin A. *J Invest Dermatol* 103:143–147, 1994b

Paus R, Handjiski B, Eichmüller S, Czarnetzki BM: Chemotherapy-induced alopecia

in mice. Induction by cyclophosphamide, inhibition by cyclosporine A, and modulation by dexamethasone. *Am J Pathol* 144:719–734, 1994c

Paus R, Schilli MB, Handjiski B, Menrad A, Henz BM, Plonka P: Topical calcitriol enhances normal hair regrowth but does not prevent chemotherapy-induced alopecia in mice. *Cancer Res* 56:4438–4443, 1996

Paus R, Foitzik K, Welker P, Bulfone-Paus S, Eichmüller S: Transforming growth factor-β receptor type I and type II expression during murine hair follicle development and cycling. *J Invest Dermatol* 109:518–526, 1997

Paus R, van der Veen C, Eichmüller S, Kopp T, Hagen E, Müller-Röver S, Hofmann U: Generation and cycling remodeling of the hair follicle immune system in mice. *J Invest Dermatol* 111:7–18, 1998

Paus R, Müller-Röver S, van der Veen C, *et al*: A comprehensive guide for the recognition and classification of distinct stages of hair follicle morphogenesis. *J Invest Dermatol* 113:523–532, 1999

Romeis B: *Mikroskopische Technik*. Munich: Urban & Schwarzenberg, 1991

Roth SI: The cytology of the murine resting (telogen) In: Lyne AG, Short BF (eds). *Biology of the Skin and Hair Growth*. Sydney: Angus and Robertson, 1965

Schilli MB, Ray S, Paus R, Obi-Tabot E, Holick MF: Control of hair growth with parathyroid hormone (7–34). *J Invest Dermatol* 108(6):928–932, 1997

Schilli MB, Paus R, Menrad A: Reduction of intrafollicular apoptosis in chemotherapy-induced alopecia by topical calcitriol-analogs. *J Invest Dermatol* 111:598–604, 1998

Silver AF, Chase HB, Arsenaut CT: Early anagen initiated by plucking compared with early spontaneous anagen. *Adv Biol Skin* 9:265–286, 1969

Slominski A, Paus R: Melanogenesis is coupled to murine anagen: toward new concepts for the role of melanocytes and the regulation of melanogenesis in hair growth. *J Invest Dermatol* 101:90S–97S, 1993

Slominski A, Paus R, Costantino R: Differential expression and activity of melanogenesis-related proteins during induced hair growth in mice. *J Invest Dermatol* 96:172–179, 1991

Slominski A, Paus R, Plonka P, Chakraborty A, Maurer M, Pruski D, Lukiewicz S: Melanogenesis during the anagen-catagen-telogen transformation of the murine hair cycle. *J Invest Dermatol* 102:862–869, 1994

Stenn K, Paus R: What controls hair follicle cycling? *Exp Dermatol* 8:229–236, 1999

Stenn KS, Paus R: Controls of hair follicle cycling. *Physiol Rev* 81:449–494, 2001

Stenn KS, Combates NJ, Eilertsen KJ, Gordon JS, Pardinas JR, Parimo S, Prouty SM: Hair follicle growth controls. *Dermatol Clin* 14:543–558, 1996

Stenn K, Parimoo S, Prouty S: Growth of the hair follicle: a cycling and regenerating biological system. In: Chuong CM (ed.), *Molecular Basis of Epithelial Appendage Morphogenesis*. Austin, TX: Landes Bioscience Publishers, 1998

Straile WE, Chase HB, Arsenault C: Growth and differentiation of hair follicles between periods of activity and quiescence. *J Exp Zool* 148:205–221, 1961

Sundberg JP: *Handbook of Mouse Mutations with Skin and Hair Abnormalities*. Boca Raton, FL: CRC Press, 1994

Weedon D, Strutton G: The recognition of early stages of catagen. *Am J Dermatopathol* 6:553–555, 1984

Wolbach SB: The hair cycle of the mouse and its importance in the study of sequences of experimental carcinogenesis. *Ann N Y Acad Sci* 53:517–536, 1951